Evaluation of Aerial Remote Sensing Techniques for Vegetation Management in Powerline Corridors

Steven J. Mills, Marcos P. Gerardo, Zhengrong Li, Jinhai Cai, Ross Hayward, *Member, IEEE,* Luis Mejias, *Member, IEEE*, and Rodney A. Walker, *Member, IEEE*

Abstract—The following paper presents an evaluation of airborne sensors for use in vegetation management in powerline corridors. Three integral stages in the management process are addressed including, the detection of trees, relative positioning with respect to the nearest powerline and vegetation height estimation. Image data, including multi-spectral and high resolution, are analyzed along with LiDAR data captured from fixed wing aircraft. Ground truth data is then used to establish the accuracy and reliability of each sensor thus providing a quantitative comparison of sensor options.

Tree detection was achieved through crown delineation using a Pulse-Coupled Neural Network (PCNN) and morphologic reconstruction applied to multi-spectral imagery. Through testing it was shown to achieve a detection rate of 96%, while the accuracy in segmenting groups of trees and single trees correctly was shown to be 75%. Relative positioning using LiDAR achieved a RMSE of 1.4m and 2.1m for cross track distance and along track position respectively, while Direct Georeferencing achieved RMSE of 3.1m in both instances. The estimation of pole and tree heights measured with LiDAR had a RMSE of 0.4m and 0.9m respectively, while Stereo Matching achieved 1.5m and 2.9m. Overall a small number of poles were missed with detection rates of 98% and 95% for LiDAR and Stereo Matching.

***Index Terms*—Vegetation Mapping, Power Transmission Lines, Stereo Vision, Laser Measurement Applications, Image Segmentation**

I. Introduction

MODERN day society relies on the widespread distribution of electricity. Whether it is in the home or office, industry or health care, over a century since its inception, electricity has found its way into almost every aspect of daily life. It is no wonder then that reliability is of the highest priority in the supply and distribution of electricity. In order to distribute electricity from power stations to consumers, electricity companies install thousands of kilometers of conductors. To avoid roads, houses and other structures, conductors are either supported overhead with the use of power poles or buried underground in protected wire looms.

Overhead lines are generally the preferred option as they are significantly easier to install and maintain. However, the bare conductors rely on the surrounding air mass for insulation and as such require sufficient separation from nearby objects including buildings and vegetation. Although man made structures can be controlled through building regulations, vegetation is naturally occurring and, particularly in rural areas, growth is unmanaged. Generally accepted as the largest cause of power failures [1], [2], a single tree falling across a power line can result in widespread outages. Storms are a major factor as they bring wet weather that weakens soil, along with strong winds that can bring branches and in some instances entire trees down onto lines. In drier regions, such as central Queensland, trees that grow up into power lines can also catch fire and spread into bushfires. This responsibility then falls upon the electricity company to periodically inspect for vegetation encroachment.

Vegetation encroachment is less of an issue in urban areas where councils and private land owners generally maintain their trees. These networks also tend to be denser, and access is made easier through public road systems, making 12-24 month inspection cycles feasible and cost effective. On the other hand, with limited access and large distances to cover, inspection cycles in rural areas see these figures extended out as far as five years. To further complicate the matter, the inspection process involves two visits, with the first used to identify spans that require clearing, followed by a second to ensure contractors have removed, or suitably trimmed, problem trees. These inspections are primarily performed on foot, driving between spans, or from a helicopter flown along side the line [3]. Neither method presents an economical or efficient solution to the problem, with on-foot patrols consuming vast man hours in travel, and helicopter inspections not only expensive, but taxing on the pilot and

Manuscript received October 7, 2009. This work was conducted within the CRC for Spatial Information, established and supported under the Australian Government's Cooperative Research Centres Programme, and sees collaboration between the Queensland University of Technology (QUT), the Australian Research Centre for Aerospace Automation (ARCAA) and Ergon Energy Australia.

S. J. Mills, L. Mejias, and R. A. Walker are with the Australian Research Centre for Aerospace Automation (ARCAA), Queensland University of Technology (QUT), Brisbane, QLD, 4001, Australia (e-mail: sj.mills@qut.edu.au; luis.mejias@qut.edu.au, ra.walker@qut.edu.au).

M. G. Castro, Z. Li, J. Cai and R. Hayward are with the Cooperative Research Centre for Spatial Information (CRCSI), Queensland University of Technology, Brisbane, QLD, 4001, Australia (e-mail: zhengrong.li@student.qut.edu.au; j.cai@qut.edu.au, marcos.gerardocastro@qut.edu.au, r.hayward@qut.edu.au).

operator [4].

Over the past two decades a number of ideas have come forth seeking to reduce this workload. These include improvements to data collection through automated camera tracking systems [5], [6], line inspection robots [7], and unmanned aerial systems [8]. In addition, a number of post processing algorithms have emerged addressing data analysis, including automated detection of vegetation [9-11], height estimation [12], [13] and feature extraction [14], [15]. As with many of these research projects, this work is closely aligned with industry, with support and collaboration from Queensland's largest supplier of electricity, Ergon Energy. With over 150 000kms of power line covering an area of 1.8 million sq. km, Ergon has one of the widest spread networks in the world and foresees significant benefit in automated inspection processes [16]. Of particular interest is automating the process of data analysis for vegetation management.

The work presented here seeks to evaluate the feasibility of extracting such information from commercial data using advanced remote sensing techniques and image processing algorithms. While the development of a specialized sensor suit has its advantages, consideration should be made to the number of units required to effectively cover the intended network. Each additional unit has its own associated costs to manufacture and maintain, while the custom nature of the installation is likely to see installation on dedicated aircraft. If however, analysis algorithms are developed to process a wide range of aerial data, then any number of commercial data provides can fly the network simultaneously, not only reducing the time taken to inspect the network, but eliminating the need for the electricity company to own and operate the inspection aircraft and/or equipment. The downside to this being that analysis algorithms must handle and interpret data from a variety of sensors. To evaluate this, two commercial aerial data providers were tasked to fly a section of line, over which one would collect high resolution and multi-spectral imagery, the other, high resolution imagery and LiDAR. Data was then post processed to extract the necessary information required for vegetation management and then compared with ground truth to provide a quantitative assessment of accuracy and feasibility. It is these findings and lessons learnt that are presented in this article.

The outline of this paper is as follows. The first section provides the reader with a summary of previous work and relevant research covering sensor options and algorithms. Experiment Methodology provides an overview of the experiment setup including the acquisition of ground truth data. This is followed by Data Collection where a description of both platform and sensor payloads flown are detailed. Analysis and Results summarize the findings of post processing and provides a quantitative comparison of techniques. Finally, Future Work highlights problem areas that need to be addressed as well as possible avenues for expansion of current system capabilities.

II. Background

The process of automatically extracting information for the purpose of vegetation management can be separated into three tasks. Initially the goal is to detect any vegetation growing within the power line corridor. Segmenting tree crowns not only defines regions of interest for subsequent processes, but also provides insight into tree size and species.

Following this, locating the horizontal position of the tree with respect to the power line is essential in determining the applicable clearance limit. Two metrics are applied in this instance, namely, along track position and cross track distance. Along track position is in place to account for line sway in winding conditions, as support from the power pole decreases towards the centre of the line thus allowing increased sway. The second metric, cross track distance, indicates the trees horizontal position with respect to the spans centre line, where zero would indicate directly underneath. Not only is this metric important in establishing if a tree may grow up into the lines, it's equally important in determining if a tree poses a threat if it were to fall or drop limbs.

The final task quantifies the level of risk by estimating the trees height and comparing it with that of the safe clearance limit derived from the trees relative position. If a tree is found to be outside the limit, it may in many instances be left alone, while a tree found to be well within the limit may prompt immediate attention.

A. Vegetation Detection

The detection of vegetation from airborne platforms is well researched particularly in the management of forests and plantations [17]. Whilst similar in concept, the task of detecting vegetation within power line corridors is complicated by the amount of ground visible from the air. Shadows, bare soil, scrub and grass all present irregularities that need to be handled by the detection algorithm.

Over the past few years, various approaches have been proposed for the segmentation of trees crowns from aerial images, or more specifically tree crown delineation [18-20]. Although many classic segmentation algorithms are applied in the RGB colour space, their effectiveness in visually complex environments is somewhat limited. A classic example is the segmentation of trees with heavy shadows, as in Figure 1, where the tree crown is segmented along with its own shadow. One prospective improvement is through the use of spectral features outside the visible spectrum [21].

Figure 1 Example of Tree Crown and Shadow

For some time, the remote sensing community has used near infrared in the classification of vegetation, utilizing distinct spectral signatures characterized by the absorption ratio of radiation in red and near infrared bands [22]. In this study, the algorithm developed by Li et al. in [23] is used for the detection and delineation of tree crowns as it has been shown to outperform both JSEG [19] and TreeAnalysis [24] in these applications. The algorithm employs a simplified Pulse Couple Neural Network (PCNN) that uses spectral features as input, post-processed using morphological reconstruction. PCNN itself is a relatively new biologically inspired approach that has been successfully applied to many image segmentation problems [25-27], and has been modified for this task with the n[th] iteration at neuron N_{ij} expressed as follows.

$$F_{ij}(n) = S_{ij} \quad \textbf{(1)}$$

$$L_{ij}(n) = \alpha_L \times \sum_{(k,l)\in K} W_{Lkl} \times Y_{kl}(n-1) \quad \textbf{(2)}$$

$$U_{ij}(n) = F_{ij}(n) \times (1 + \beta \times L_{ij}(n)) \quad \textbf{(3)}$$

$$Y_{ij}(n) = \begin{cases} 1 & U_{ij}(n) > \Theta_{ij}(n) \\ 0 & other \end{cases} \quad \textbf{(4)}$$

$$\Theta_{ij}(n) = \begin{cases} \Theta_{ij}(n-1) - step \\ V_t \times V_a \quad if\ Y_{ij}(n-1) \neq 0 \end{cases} \quad \textbf{(5)}$$

Where n is the iteration number; F and L the feeding and linking part respectively, while S_{ij} is the external stimulus from the feeding field. U is the internal activity of neurons; Y is the pulsed output of neurons; W_L is the linking weight matrix which is the reciprocal of the Euclidean distance between the center of window and the other window elements; K is the size of the window which is put on a neuron; α_L is the linking scale; V_t is the threshold magnitude scale which is larger than 1 ; V_a is the maximum value of the input image; β is the linking strength, set to 0.2 for this study; Θ is the dynamic threshold matrix which controls whether the neuron can impulse or not; $step$ is the decay coefficient and Y_a is the accumulation of previous output.

External stimuli S of the neurons are calculated from the feature space using spectral band ratio,

$$S = \rho_{NIR} / \rho_{red} \quad \textbf{(6)}$$

Where ρ_{NIR} and ρ_{red} are the spectral reflectance of NIR and red band respectively. Due to the strong absorption contrast between NIR and red band in trees, the corresponding neurons have greater external stimuli and thus pulse more frequently. It should be noted that this ratio takes the form of the vegetation index, Ratio Vegetation Index (RVI) [28]. Although other vegetation indexes could have been used, including the well known Normalized Difference Vegetation Index (NDVI), RVI was found to better suit the problem, maximizing the contrast between vegetation and non-vegetation. An example of this is shown in Figure 2, where NDVI and RVI outputs are shown for the same multi-spectral image.

By accumulating pulse outputs, a threshold can be applied to segment tree foliage from background pixels. Noise and discontinuities may result from this process requiring post processing to delineate the whole crown. A basic morphological opening operator and reconstruction filter can be used at this stage to reduce noise and fill holes respectively.

B. Relative Positioning

Given that a tree has been automatically identified within the powerline corridor, it is important to establish the horizontal position with respect to the line. As previously mentioned, clearance requirements vary both along the line and perpendicular to the span centre line. It is important that an accurate estimate is made as the clearance limit will determine if a tree is trimmed or removed and the equipment required to carry out the job [29].

Of the sensors under consideration both image based and LiDAR can be used to acquire this information. As vegetation detection takes place in multi-spectral images, it is advantageous if the imaging sensor can be utilized for relative positioning. Direct observations obtained from GPS and INS can be used in conjunction with standard approaches used in geo-referencing [30], [31]. For simplicity, the basic equation is recalled here

$$r_t^m = r(t)_{gps}^m + R(t)_b^m [\, s_i R_c^b r(t)_t^c + a^b \,] \quad \textbf{(7)}$$

Where, $r(t)_{gps}^m$ is the vector containing the coordinates of the INS center in the mapping frame; $R(t)_b^m$ is the attitude matrix from the INS body frame to the mapping frame; s_i is a scale factor between the image and mapping coordinates frames for a specific point (i); R_c^b is the rotation matrix between the camera frame and the INS body frame; r_t^c is the vector of coordinates observed in the image frame for the point of interest; and a^b is the vector of the translation offset between the INS and the camera centre in the INS body frame.

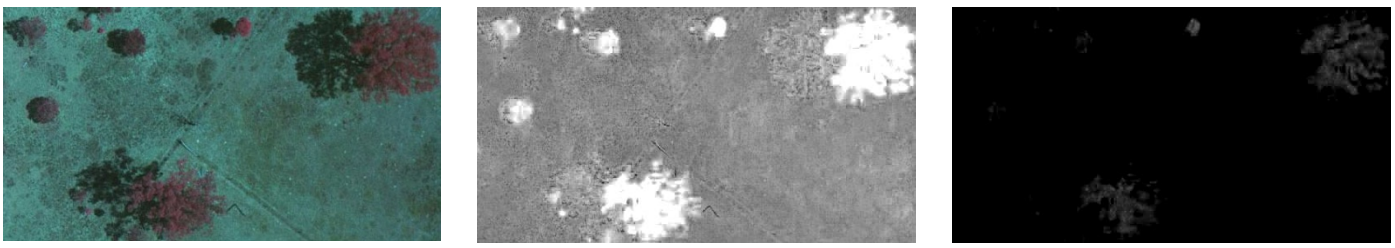

(a) Colour-Infrared (CIR) (b) RVI (c) NDVI

Figure 2 Comparison of RVI and NDVI

In essence, direct geo-referencing (DG) takes a point in the image plane and maps it to an inertial reference frame using the absolute position of the GPS antenna and the orientation of the aircraft as registered by the INS in the body frame.

Low precision DG systems typically assume alignment between sensor axes, however for more detailed work, compensation for relative positioning and alignment is essential. Boresight misalignment, displacement between GPS and INS and the topography of the earth surface are all important factors that must be taken into consideration [32].

The second means of acquiring relative distances to be tested is that of LiDAR. Although principally designed for acquiring precise range information, these systems are typically coupled with positioning sensors when used in aerial surveying to create digital elevation models [10], [11], [32]. Thus with absolute position information available, relative positions can be derived.

C. Height Estimation

The final step in extracting data for vegetation management is automatically estimating the height of trees. Ultimately the decision to remove a tree and the technique used is governed by the overall clearance from the line as estimated by the height. Much the same as with relative positioning, both LiDAR and image sensors potentially capture this information.

A popular method used in the estimation of heights and depths, in both computer vision and photogrammetry, is that of stereo matching [1], [13], [33], [34]. Two recent papers applying these techniques to vegetation management include those by Sun et al. in 2006 and Kobayashi et al. in 2009 [1], [9]. Sun et al. successfully detect power poles and estimate the height of vegetation using stereo images captured from a low flying fixed wing aircraft. Although the output of stereo matching and mosaicking is shown through a series of figures, no quantitative evaluation of accuracy is presented. Kobayashi et al. apply similar techniques to multi-spectral image pairs of satellite images, focusing on the detection and measurement of vegetation within the power line corridor. Again a series of images are provided to illustrate the ability of the algorithm to estimate height, but no quantitative evaluation of the accuracy is reported.

The basic principal governing stereo matching comes from the relative disparity generated when an object is viewed from two vantage points. It can be shown through trigonometry that this relative disparity is proportional to the depth of object viewed. Typically two cameras are used and disparity is generated through *physical* separation, however taking two pictures from a single moving camera has the same effect, where disparity is generated in the *time* domain.

Over the past two decades there have been a vast number of algorithms to come forth including Graph-Cut [35] and Belief Propagation [34] which are widely accepted as accurate methods. This accuracy however comes at a cost. Inherently computationally inefficient these algorithms do not offer a realistic solution on the scale of processing required for this application [34].

Another widely used method that offers the computation efficiency required for this application is Dynamic Programming over scan lines [36]. Well known as handling low-contrast scenes, traditional dynamic programming finds the path with lowest matching cost between scan lines taken from each image. As traditional dynamic programming cannot estimate the disparity in occlusion regions, an improved algorithm is proposed, which can be summarized over the following 4 steps:

Step 1: Initialization

$\alpha(i,d) = 2cost(i,d), i = 0$ and $\min D \le d \le \max D$

$path(i,d) = 0;$

Step 2: Recursion. From time i=1 to N-1.

$$\alpha(i,d) = min_k \begin{Bmatrix} \alpha(i-1,k) + cost(i,d) + O_1(i,k,d) & \text{if } k < d \\ \alpha(i-i,k) + 2cost(i,d) & \text{if } k = d \\ \alpha(i-k-d-1,k) + cost(i,d) + O_2(i,k,d) & \text{if } k > d \end{Bmatrix}$$

$$path(i,d) = k$$

Step 3: Termination

$d_{N-1} = arg\, min_d \{\alpha(N-1,d)\};$

Step 4: Path backtracking. From time i=N-2 to 0.

$d = path(i+1, d_{i+1});$

$i = i - (d_{i+1} - d) - 1;$

$d_i = d;$

Where i is the pixel index of the second scan line, $\alpha(i,d)$ is the accumulated matching cost at ith pixel with a disparity d, the disparity range is from *minD* to *maxD*, $cost(i,d)$ is the matching cost, $O_1(i,k,d)$ and $O_2(i,k,d)$ are matching costs of the left and right occlusion respectively.

The alternate solution to Stereo Imagery is LiDAR [13]. As previously discussed, LiDAR sensors are primarily used in detailed digital elevation modeling making it a convenient option for height estimation. However due to the discrete nature of the sensors operation, sending only a few pulses per square meter, objects with small cross sectional areas including branches, sparse trees, power poles and power lines are potentially missed [37]. Although imaging sensors are equally restricted by spatial resolution, small features may still be detected given sufficient contrast between the object and its surroundings.

III. Experiment Methodology

To evaluate the techniques discussed previously, two experiments where developed. The first experiment would assess segmentation techniques for tree crown delineation within powerline corridors. The second would evaluate the accuracy and reliability of detecting and measuring the relative location and height of vegetation in proximity to power lines with both image data and LiDAR.

A. Tree Crown Delineation

Criterion for successful vegetation detection in this study is defined as an individual tree having been delineated whilst

preserving the contour of the crown. In order to produce a quantitative evaluation, an analysis of under-segmentation and over-segmentation was conducted using a set of four metrics: 1-to-1, 1-to-M, M-to-1 and missing [38].

The first criterion, 1-to-1, indicates the successful mapping of a single tree crown in the real world to a single tree crown by the segmentation algorithm. 1-to-M defines a single tree crown that has been incorrectly segmented into several portions, likewise M-to-1 describes a cluster or group of trees that have been segmented as one. Finally those trees that are misclassified as background are classified as missing. The accuracy of any algorithm is then calculated as the proportion of correct 1-to-1 mappings to the total number of trees present. In certain instances it will be necessary to inspect vegetation from the ground to acquire an accurate truth data set.

B. Location & Height Estimation

As previously discussed, the relative location of a tree with respect to a powerline can be defined by two metrics, along track position and cross track distance. The first measure indicates the relative position of the tree with respect to the length of the span and is usually given as a ratio. The second describes the perpendicular distance from the line, or cross track distance, and is specified in meters. To obtain these measurements requires establishing the absolute location of both the tree and two adjoining poles and applying simple geometric equations to resolve relative positions. To remove position and orientations errors, ideally data would be collected on the same platform, using common positioning and attitude sensors. Truth data for this section of the experiment can be collected through a standard geographical survey.

Absolute position of the tree would be taken at the base to avoid ambiguity between those that grow at an angle or split. In terms of height, this was defined as the perpendicular distance from the tree base to the highest portion of foliage. For small trees, truth data can be collected using a measuring staff, however for those trees where this is infeasible a geometrical method was used as depicted in Figure 3.

Heights were then post processed using the following;

$$H_T = \frac{S_D \sin(\theta_B - \theta_T)}{\sin \theta_T} + H_S \quad \textbf{(8)}$$

Where S_D is the slant distance measured to a surveying prism held at the base of the tree; θ_B is the vertical declination to the base; θ_T is the vertical declination to the top of the tree as observed from the measurement point; and H_S is the height of the staff including prism.

The process itself can be ambiguous, particularly for acute angles of θ_T, where the top branches may not be visible. Figure 3 illustrates the worst case were a relatively flat tree crown has limbs spreading outwards. From this particular observation point the *top* of the tree would be identified as Point A, as apposed to actual top at Point B. This results in over estimation of the height. The error can be expressed through the following relationship, where C_R is the crown radius;

$$H_E \le C_R \cot(\theta_T) \quad \textbf{(9)}$$

Hence, moving the observation point away from the tree and onto elevated ground should minimize this source of measurement error. Even so, a small amount of uncertainty will still exist in any tree height measurement. To resolve this ambiguity it was decided to include pole heights in the experiment as they have a clear and well defined top, providing an unambiguous test case to measure performance against.

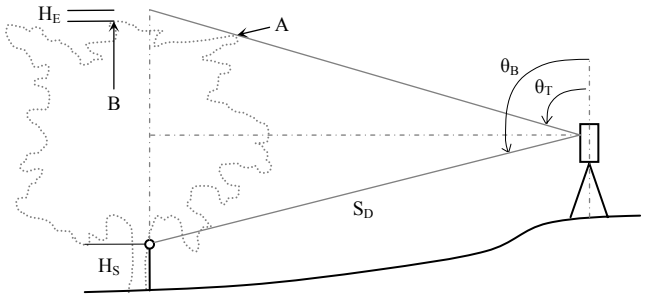

Figure 3 Obtaining Truth Data for Tree Heights

IV. Data Collection

Data collection for this study included gathering aerial data for sensor evaluation, as well as conducting a ground survey for verification. A 1.5km section of line spanning between the rural towns of Murgon and Wondai in South East Queensland, Australia, was selected as the test site. Figure 4 shows a mosaic of the test area generated from aerial images acquired from the trial, where white lines indicate power lines and dashed lines those outside the test area.

To coordinate the ground survey, control points were established at either end of the test area using Trimble 5700 L1/2 GPS Receivers fitted with Zephyr Geodetic Antennas. Six hour observation sessions were used at each site with subsequent GPS RINEX files submitted to the AUSPOS GPS Processing Service to obtain 20mm accurate coordinates in the International Terrestrial Reference Frame (ITRF) & the Geocentric Datum of Australia (GDA). A Topcon GTS-6A Total Station was then used for traversing and measuring the parameters for height estimation as detailed in §III.B. In total, 44 poles and 33 trees were surveyed in the designated test site.

A. Aerial Data

As no single provider could capture the full range of sensor data required for the experiment, two separate providers were contracted to collect data over the test site.

1) Provider of LiDAR & High Resolution

The first provider of data was a Queensland based company that supplies aerial mapping, LiDAR and other GIS services to government and industry. The system consists of an Integrated LiDAR and Digital Photography System mounted in the cargo area of a modified Cessna U206G shown in Figure 5 (left).

Figure 4 Experiment Test Site

The main sensors onboard the aircraft include;

1. TopoSys Harrier 56 Full Wave LiDAR Scanner
2. Rollie 39 mega-pixel Camera
3. Applanix POS/AV 410 Inertial Motion System
4. 12 Channel Dual Frequency DGPS

The flight for data collection occurred on the 9th of December 2008, during which the aircraft was flown at approximately 55m/s (106kts) at an altitude of 500m AGL yielding spatial resolution or ground sample distance (GSD) of 10cm. As the aircraft was not set up for stereo cameras, disparity for stereo matching would come from overlap in successive frames. This necessitates that overlap between frames falls no less than 50%. LiDAR data was collected at 200kHz, with a scan angle of ±30º with an average sample rate of 9 points per square meter.

2) Provider of Multi-Spectral & High Resolution

The second series of flights occurred earlier on the 25th of November 2008 by another local company. Contracted to collect multi-spectral data, their system consists of a DuncanTech MS-4100 multi-spectral camera with DGPS/INS as well as higher resolution natural colour Canon 1Ds Mark III 22MP camera. This equipment is mounted in the cargo area of a Piper Cub as pictured in Figure 5 (right).

Multi-spectral data is captured over 4 spectral bands: NIR (800-966nm), red (670-840nm), green (540-640nm), blue (460-545nm). Traveling at approximately 34m/s (65 knots) and an altitude of 350m AGL, images were captured at approximately 15cm GSD for multi-spectral and 5cm for high resolution. As with the first provider, overlap for stereo imagery would be produced by subsequent frames as the aircraft could not carry two cameras with sufficient baseline.

V. Analysis & Results

The aim of the following analysis is to quantitatively assess each of the sensors and their feasibility for vegetation management. For this, data collected from the flight trials was post processed using techniques described earlier and the results compared to ground truth.

A. Tree Crown Delineation

Of the multi-spectral images captured, a series of nine were selected for processing. Frames were removed from the full sequence of images to minimize overlap that would see some trees processed more than once. Further more, the algorithm was only applied to those areas of the image that contained the powerline corridor. Figure 6 shows an example of the automatic tree segmentation algorithm (white) discussed in §II.A overlaid with manual segmentation (red) verified through ground truth. Visually one can see that the automated segmentation algorithm has successfully detected and removed shadow from all trees present.

Analysis results for the nine images are shown in Table 1. *Img* indicates the image number and *Truth* indicates the number of trees in the region of the image. As previously described, *1-to-1* indicates successful segmentation where a single tree is segmented as one crown, whereas *1-to-M* and *M-to-1* indicate an error where a single tree has been subdivided or a group of trees joined together in the segmentation process. *Missing* indicates that a tree has been misclassified as ground.

Figure 5 Data Collection Systems

Table 1 Results of Automated Tree Crown Segmentation

Img	Truth	1-to-1	1-to-M	M-to-1	Missing	Accuracy
1	21	13	0	6	2	61.9%
2	11	11	0	0	0	100%
3	25	14	1	8	0	56%
4	21	20	1	0	0	95.2%
5	11	8	1	2	0	72.7%
6	15	10	0	4	1	66.7%
7	3	3	0	0	0	100%
8	11	10	0	0	1	90.9%
9	11	8	0	2	1	72.7%
	129	97	3	22	5	75.2%

Two examples of these errors can be seen on closer inspection of Figure 6, (1) where two trees growing close to one another have been segmented as one and (2) where a small tree has been missed. Of these errors, trees missed by the algorithm are of greatest concern as it is at this stage that candidate trees are selected for further processing. Although over and under segmentation is undesired, detection is achieved all the same, whereas those missed by the algorithm are potential threats that go unchecked. It appeared that sparse foliage and small crowns were the main source of error, where the combination of low spatial resolution and low foliage density produced limited contrast for segmentation. Overall 124 of 129 trees imaged were detected thus yielding a detection rate of 96%.

With regards to correct segmentation, the algorithm was found to achieve an accuracy of 75.2%, with the main contribution of error stemming from under segmentation. Even to the naked eye these instances are hard to detect as under segmentation typically occurs when trees have grown in a tight group and have overlapping crowns. Add to that clusters containing similar species and the problem is further complicated with similar colors and even texture.

B. Relative Positioning

The second series of experiments were developed to investigate the accuracy and reliability of relative positioning from two common techniques, direct georeferencing of image data and LiDAR. Using the techniques described in §II.B and images acquired by the Rollie 39MP camera, poles and trees were directly georeferenced (DG) into GDA coordinates. Identifying a trees base from overhead imagery is however complicated by the crown which obstructs the base from view. For this experiment, these locations were estimated manually. Having resolved the absolute position of both poles and trees, simple trigonometric identities were then applied to compute both cross track and along track measurements.

Extracting the same information from LiDAR required less computation as proprietary software (MARS® Viewer) post processes raw data automatically to obtain absolute positions. LiDAR is also able to penetrate the trees foliage allowing the base to be easily identified. After manually identifying poles and trees, similar methods were then used to calculate relative cross track and along track distances.

Table 2 shows results of absolute positioning for both LiDAR and DG compared with truth data. Error in this instance is calculated as the horizontal distance from the true location to the measured. As can be seen, the accuracy of LiDAR in both instances is higher than that of DG. Interestingly errors for both LiDAR and DG were reduced for

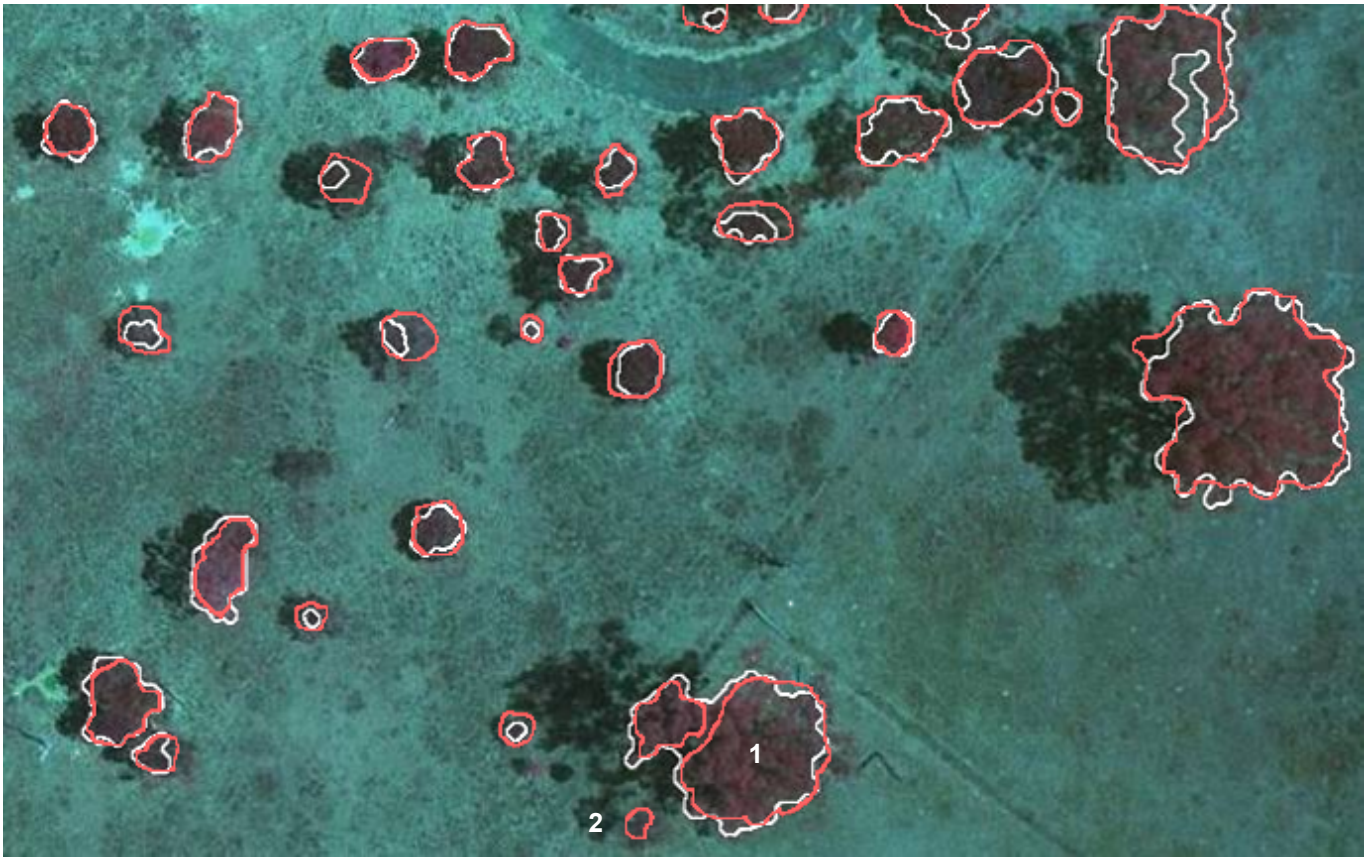

Figure 6 Tree Crown Delineation Results (Manual - Red, Automatic - White)

Trees, however at best one would expect the same, if not reduced, accuracy as a degree of uncertainty is present when determining the base of a tree from above. From the results as well as random errors on the DG measurements, a small amount of bias was present indicated by the average error being larger than the standard deviation. In any case these errors where within expectation and of more concern was the use of these measurements for relative positioning.

Table 2 Absolute Positioning Results for LiDAR and Image Georeferencing

	Poles		Trees	
	LiDAR	Image	LiDAR	Image
Sample Size	44		33	
Average Error	1.0 m	2.9 m	0.8 m	2.4 m
Standard Deviation	1.0 m	1.3 m	0.4 m	1.2 m
Worst case	2.2 m	5.2 m	1.9 m	5.1 m

With absolute positions established for both poles and trees, relative distances can be processed. It was expected that accuracy would improve as common errors coupled in the absolute positioning calculations would cancel. Table 3 shows the results of relative positioning, where cross track error refers to the error in estimating the perpendicular distance to the line and along track error, the error in measuring the distance from the closest pole.

Table 3 Relative Positioning of Vegetation with LiDAR and Image Georeferencing

	Cross Track		Along Track	
	LiDAR	Image	LiDAR	Image
Average Error	0.2 m	0.7m	-0.1 m	-1.3 m
Standard Deviation	1.4 m	3.1m	2.1 m	3.1 m
Worst case	6.2 m	8.2 m	4.7 m	3.3 m
Sample Size	30			

While accuracy improved, precision decreased across the board for both methods. This would possibly infer that while common errors cancelled, that noise in the first measurements coupled introducing further uncertainty. Once again the accuracies achieved by LiDAR surpassed that of image based techniques, however neither would be unacceptable in this application as long as this uncertainty was taken into consideration.

Overall, LiDAR demonstrated accuracy and reliability well over that of direct georeferencing techniques. With a 95% confidence interval results showed LiDAR cross track measurements could be measured to 0.2±2.8m while georeferencing was found to be 0.7±6.2m, likewise along track was found to be -0.1±4.2m and -1.3±6.2m. It is worth noting that both LiDAR and image data for this experiment were collected from the same platform, during the same flight and utilized the same DGPS and INS unit. Hence although improvements to position and attitude data theoretically improve these results, the same margin of accuracy between the methods would be expected.

C. Height Estimation

The final series of experiments were developed to evaluate sensor options available for the estimation of heights. As detailed in §II.C, both imaging and LiDAR sensors were identified as potential sources of information, with image data requiring post processing.

A total of 44 poles were surveyed in the test area and were selected for this experiment to serve as an unambiguous test case for height estimation. Unlike trees that can be somewhat ambiguous, poles have a clearly identifiable base and apex.

Height estimation from LiDAR data was performed manually by selecting a suitable return from the top of the pole and subtracting the average return height from the ground. One problem found whilst processing LiDAR data was the lack of returns from poles. This can be attributed to the relatively small cross sectional area presented from a top view. Although the majority of poles had at least one or more returns, some poles were completely missing with only returns from the ground surrounding the base. This problem can in some ways be resolved through the interpolation of LiDAR returns from conductors leading up to and away from the pole, however height data of the pole is forever lost. Of the 44 poles

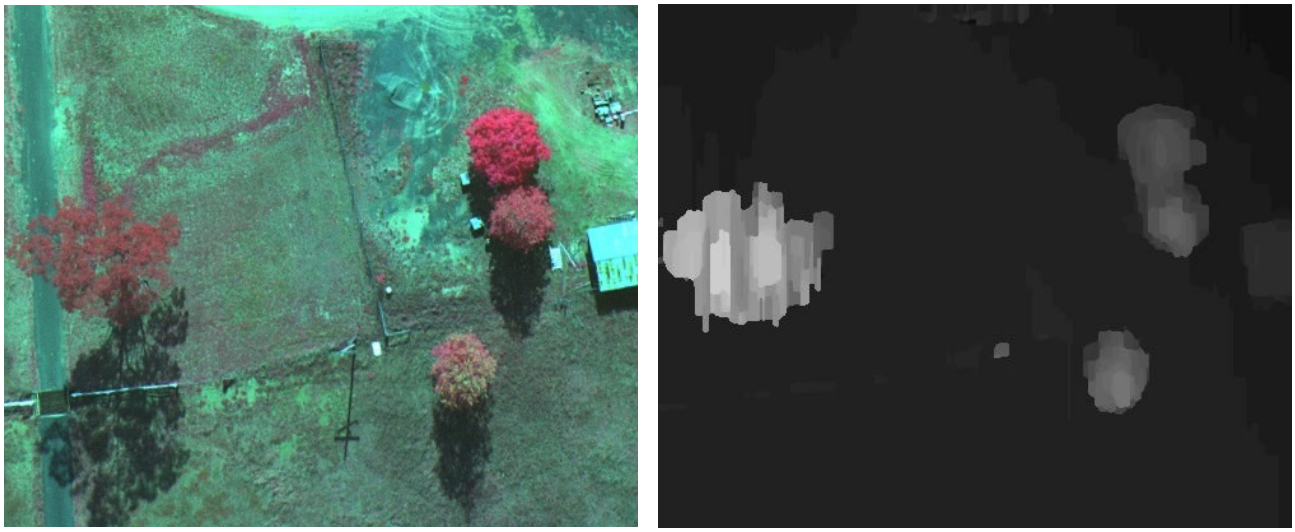

(a) Original Multi-Spectral Image (b) Stereo Image Depth Map

Figure 7 Height Estimation using Stereo Matching

that were surveyed in the test area, LiDAR returned responses for 43 poles, yielding a detection rate of 98%.

Height estimation from image data required post processing using the stereo matching algorithms described in §II.C. Figure 7 shows an example of the depth maps generated by the algorithm using the multi-spectral images. Intensity of the map pixels symbolize an increase in height from black to white. Processing was attempted on all three data sets that were collected, however a number of issues were encountered. The first issue arose with the image data acquired by the high resolution Rollie 39MP camera. Due to factors outside the control of the experiment, data provided had less than the 50% overlap. Without this overlap two views of each object can not be guaranteed as is required for stereo matching.

The second set of data acquired from the multi-spectral sensor was also found to be less than ideal. Captured with the highest percentage of overlap, the spatial resolution was found to be too low to reliably detect the poles during the matching process. Even to a human observer, 15cm resolution results in 2-4 pixels per pole which is in most cases renders the object undetectable against a complex background.

The final set of data captured from the Canon 1Ds Mark III 22MP with the highest level of spatial resolution, was found to be more than sufficient for the matching process. Only in one instance was the overlap an issue where half a pole was seen in one frame and the other half in another, hence reinforcing the importance of overlap. Of the 44 poles selected for the experiment, 2 were missed due to this issue above, while a further two fell outside the swath of the camera. This left 40 poles, of which 38 were successfully matched by the algorithm, yielding a detection rate of 95%.

In one case it was found that the angle of the sun had been such that one side of the pole was completely illuminated whist in the subsequent frame completely in shadow. Imaging each object three times can prevent this problem, guaranteeing the object is captured twice on the same side. Practically this can be achieved by setting the flight parameters in such a way to achieve overlap of 67% or more.

Table 4 Results for Power Pole Height Estimation

	LiDAR System	Stereo Matching
Detection rate	95.4%	95.0%
Sample Size	44	40
Average error	0.3 m	1.1 m
Standard deviation	0.4 m	1.5 m
Worst case	1.5 m	4.7 m

Results for this experiment are presented in Table 4. The average error is calculated as the ground truth for each pole minus the estimated height and averaged over all measurements. Likewise, the standard deviation is calculated on those same error terms. We see that both the average and standard deviation of the error for LiDAR is over three times better than that of Stereo. Although in some ways represented by the standard deviation, analysis of the data shows only 3 instances of gross error on the order of 1.5m, in all other cases the error is below 0.5m. This could possibly be accounted as the return coming from the cross bar on the pole as apposed to the very top. Stereo unfortunately did not show as much promise. A number of gross errors were present, including three instances of underestimation greater than 4m.

Of the poles that were missed, only one was common to both. Hence an overall detection rate of 98% could be achievable through the integration of data sets. So although merit may not exist for the use of stereo imagery in height estimation, it may prove beneficial to integrate both sensors to supplement misdetection.

The second series of experiments looked at the accuracy and reliability of estimating the height of trees. As with poles, LiDAR data was manually analyzed, with the height of trees determined by the highest return from the top of the tree minus the average return from the ground. Stereo matching algorithms were once again applied to both high and low resolution data for a comparative analysis.

An issue not encountered whilst measuring poles arises from the trees base which is not visible in the stereo image depth map due to the trees crown. To work around this issue, an estimate was made by taking the median of four neighboring points, equally spaced just outside the tree crown. As to be expected, the spatial resolution requirements for vegetation were found to be significantly less than that of poles, with 15cm GSD found to be more than adequate for accurate matching. A new issue however was encountered during the analysis of the higher resolution data captured by the Canon 1Ds Mark III. In certain instances, even with sufficient overlap, matching results were found to contain increased levels of noise.

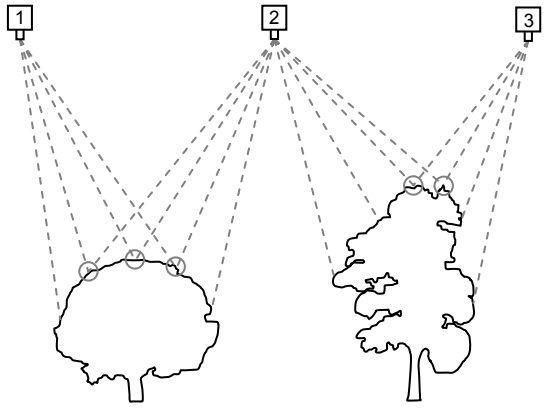

Figure 8 Matching Limitations due to View Angle

Further analysis revealed that due to a decrease in frame rate, recalling that these sensors where flown on the same platform, the high resolution image pairs had a longer baseline that introduced distortion to the imaged tree crown. To illustrate this distortion, Figure 8 shows three consecutive frames taken over two trees. The first tree when imaged from stations 1 and 2 would appear similar as many of the features are seen from both positions. The second tree however, when imaged from stations 2 and 3, would appear distinctly different as opposite sides of the tree are captured.

One solution is to capture data at higher altitudes where the change in view angle has less effect on an objects shape.

Unfortunately this would have a negative impact on the spatial resolution which is already at the limit of detecting poles. An alternate solution is to increase the overlap between frames, in much the same way for power poles, to ensure each tree is imaged three times. Multi image matching techniques can then also be used to improve accuracy [39]. Figure 9 illustrates this concept whereby increased overlap delivers more common points between frames.

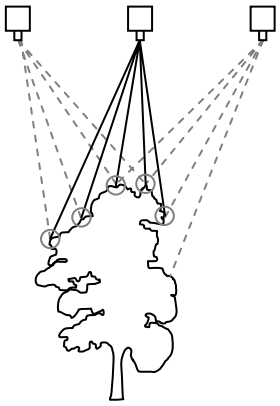

Figure 9 Improved Matching through Increased Overlap

Table 5 shows the results of tree height estimation. Once again LiDAR was found to be over 3 times as accurate and reliable as Stereo Matching. Accuracy was down in both instances with respect to pole height estimates, although this was to be expected as truth data included uncertainty in the measurements.

Table 5 Results of Tree Height Estimation

	LiDAR System	Stereo Matching
Detection rate	100% (33/33)	100% (33/33)
Sample Size	33	
Average error	0.4 m	1.8 m
Standard deviation	0.9 m	2.9 m
Worst case	-3.5 m	10.9 m

Although LiDAR was found to be relatively consistent with most errors under 1m two unexplained gross errors were discovered (3m and -3.5m). Stereo on the other hand had a number of large errors with 21 of the 33 measurements over 1m in error. A number of these errors could be attributed to the lack of contrast in the multi-spectral images between the ground cover and the tree crown. Figure 10 illustrates such a case where the stereo matching algorithm significantly underestimates the height of tree number 2. Although sufficient contrast can be seen between the trees in the first group, the second is extremely similar to that of the ground cover on the right and subsequently produces errors in the stereo matching process.

Overall it was found that LiDAR yielded superior accuracy compared to that of Stereo Matching. General improvement may be seen in LiDAR as sensor technology improves and the number of points per square meter increase as with Stereo Matching could be improved with increased overlap between frames. However it is unlikely that Stereo Matching can be improved to the point were it matches LiDARs accuracy and reliability. Although some merit exists in combining both data sets to increase detection rates.

VI. Future Work

Field trial results have demonstrated considerable merit in favour of commercially available sensors in the acquisition of data for vegetation management. Development is however an on going process, with future work set to improve performance and expand upon current capabilities.

Improving detection rates and segmentation accuracy is particularly important as it at this stage that trees are selected for further processing. Areas of low contrast in multi-spectral imagery are a significant issue that may be resolved through the inclusion of height information. Having successfully achieved tree crown delineation, focus can then turn to the classification of individual tree species. A key goal in the long term management of vegetation within power line corridors is to promote species with a mature height of less than 4m. Overtime this would create a system that self-manages the growth of undesired species through competition with desired species.

In terms of relative positioning and height estimation, LiDAR in both instances was found to be significantly more accurate and reliable when compared to image based techniques. Although improvement in reliability may be

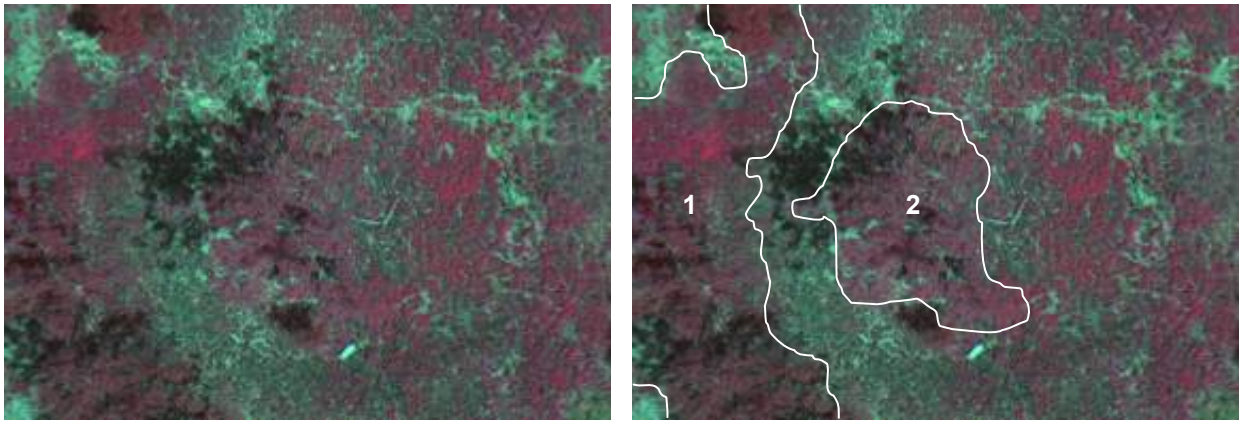

(a) Original Multi-Spectral Image (b) Segmented Tree Crowns

Figure 10 Example of Limited Contrast between Tree Crown and Background

achievable through integration of sensors data, this would come at a cost to complexity.

Although manual feature extraction has been used throughout this experiment for LiDAR, over a large data set this can become particularly time consuming. Future work will endeavor to automate this process through feature extraction, much of which can be based on pre-existing algorithms [10].

Another topic for future research concerns the influence of reduced cross sectional area for those poles without cross arms. In a number of instances cross arm returns were the only means of identifying a poles location as returns were limited by the poles surface area. As only 3 poles within the test area were without cross arms, no conclusive analysis could be drawn, however as, the only pole missed was without a cross arm prompts further investigation. This is of particular concern in regional areas where extensive use of Single Wire Earth Return (SWER) is used which require no cross arm.

A final discussion point not previously raised is the acquisition of data. Although data acquisition from fixed wing platforms has shown merit in this application, flying at low altitudes whilst maintaining the power line in the field of view of onboard sensors is a demanding job. Navigating a discontinuous feature presents further difficulties, with the typical approach to loop back around and reconnect with a line when it changes direction. On a higher level, path planning required to efficiently cover large networks is at present a problem waiting to be solved.

Automated guidance and path planning has the potential to solve these problems and provide a long term solution. Whilst work exists in this area, research is far from a practically operational system. From semi-automated solutions that provide pilots with a synthetic vision display to assist in navigating the network, to fully automated data collection systems through the use of Unmanned Aerial Systems, the options are limitless.

VII. Conclusion

In this paper the accuracy of extracting metrics for vegetation management within powerline corridors using commercially available data was evaluated. Three principal tasks in the management of vegetation were selected for the experiment; vegetation detection, relative positioning and height estimation. Through the use of a PCNN based segmentation algorithm, a detection rate of 96% was achieved in multi-spectral imagery. Trees with sparse and small crown areas were a major factor in misdetection, where a combination of low spatial resolution and low foliage density produced limited contrast for segmentation.

LiDAR and image based techniques were then applied to determine the relative position and height of candidate trees. As has come to be expected in industry, LiDAR delivered superior accuracy and reliability over that of image based techniques and would be recommended given budget and payload capability allow. Image based techniques do however have their place, with reduced cost, size and weight, they provide an alternate solution where LiDAR may be impractical, for example line inspection robots and unmanned aerial systems.

Of major concern were those poles missed by both LiDAR and Stereo Matching. Although detection rates of 98% and 95% were achieved respectively, extrapolating these figures out over a network with an estimated 1 million poles could see hundreds if not thousands of poles missed. LiDAR detection rates may improve through increased point density and inferring pole location from power line modeling, while higher overlap in stereo image pairs may see improved performance from stereo matching. These however offer marginal improvements at best, while data fusion offers far greater potential of increasing detection rates through the combination of LiDAR and Stereo.

Acknowledgments

The authors would like to thank Isaac Stiller from the Queensland Governments Department of Natural Resources and Water for his support and assistance in conducting the ground survey. In addition, the authors would like to thank Geosciences Australia for free use of AUSPOS GPS Processing Service.

References

[1] C. Sun, R. Jones, H. Talbot, X. Wu, K. Cheong, R. Beare, M. Buckley, and M. Berman, "Measuring the distance of vegetation from powerlines using stereo vision," *ISPRS Journal of Photogrammetry and Remote Sensing,* vol. 60, pp. 269-283, 2006.

[2] R. Novembri, "Utility vegetation management - final report," Federal Energy Regulatory Commission United States Government March 2004.

[3] D. I. Jones and G. K. Earp, "Requirements for aerial inspection of overhead electrical power lines," in *Proceedings of the 12th International Conference on Remotely Piloted Vehicles*, Bristol, 1996.

[4] C. C. Whitworth, A. W. G. Duller, D. I. Jones, and G. K. Earp, "Aerial video inspection of overhead power lines," *Power Engineering Journal,* vol. 15, pp. 25-32, February 2001.

[5] I. Golightly and D. Jones, "Corner detection and matching for visual tracking during power line inspection," *Image and Vision Computing Journal,* vol. 21, pp. 827-840, 2003.

[6] D. I. Jones, C. C. Whitworth, G. K. Earp, and A. W. G. Duller, "A laboratory test-bed for an automated power line inspection system," *Control Engineering Practice,* vol. 13, pp. 835-851, July 2004.

[7] K. Toussaint, N. Pouliot, and S. Montambault, "Transmission line maintenance robots capable of crossing obstacles: State-of-the-art review and challenges ahead," *Journal of Field Robotics,* vol. 26, pp. 477- 499, 23 March 2009.

[8] D. Jones, I. Golightly, J. Roberts, K. Usher, and G. Earp, "Power line inspection - a uav concept," in *The IEE Forum on Autonomous Systems*, London, United Kindom, 2005, p. 8.

[9] Y. Kobayashi, G. G. Karady, G. T. Heydt, and R. G. Olsen, "The utilization of satellite images to identify trees endangering transmission lines," *IEEE Transactions on Power Delievery,* vol. 24, pp. 1703-1709, July 2009.

[10] J. Reitberger, C. Schnörr, P. Krzystek, and U. Stilla, "3d segmentation of single trees exploiting full waveform lidar data," *ISPRS Journal of Photogrammetry and Remote Sensing,* In Press.

[11] P. Axelsson, "Processing of laser scanner data - algorithms and applications," *Journal of Photogrammetry & Remote Sensing* vol. 54, pp. 138-147, 1999.

[12] G. Yan, J. Wang, Q. Liu, L. Su, P. Wang, J. Liu, W. Zhang, and Z. Xiao, "An airborne multi-angle power line inspection system," in *IEEE International Geoscience and Remote Sensing Symposium*, 2007.

[13] B. St-Onge, C. Vega, R. A. Fournier, and Y. Hu, "Mapping canopy height using a combination of digital stereo-photogrammetry and lidar," *Int. J. Remote Sens.,* vol. 29, pp. 3343-3364, 2008.
[14] G. Yan, C. Li, G. Zhou, W. Zhang, and X. Li, "Automatic extraction of power lines from aerial images," *IEEE Geoscience and Remote Sensing Letters,* vol. 4, pp. 387-391, 2007.
[15] R. A. McLaughlin, "Extracting transmission lines from airborne lidar data," *IEEE Geoscience and Remote Sensing Letters,* vol. 3, pp. 222-226, 2006.
[16] J. Bangay, "Project 6.7: "The ergon project" - project plan," Ergon Energy 2007.
[17] D. S. Culvenor, "Extracting individual tree information: A survey of techniques for high spatial resolution imagery," in *Remote sensing of forest environments: Concepts and case studies*, M. A. Wulder and S. E. Franklin, Eds. Boston: Kluwer Academic Publishers, 2003, pp. 255-277.
[18] A. Watt and F. Policarpo, *The computer image*: Addison Wesley, 1998.
[19] Y. Deng and b. s. Manjunath, "Unsupervised segmentation of color-texture regions in images and video," *IEEE Transactions on Pattern Analysis and Machine Intelligence,* vol. 23, pp. 800-810, August 2001.
[20] Y. Wang, Y. S. Soh, and H. Schultz, "Individual tree crown segmentation in aerial forestry images by mean shift clustering and graph-based cluster merging," *IJCNS International Journal of Computer Science and Network Security,* vol. 6, pp. 40-45, November 2006.
[21] Z. Li, R. Hayward, J. Zhang, and Y. Liu, "Individual tree crown delineation techniques for vegetation management in power line corridor," in *Digital Image Computing: Techniques and Applications (DICTA)*, Canberra, 2008, pp. 148-154.
[22] R. B. Myneni, F. G. Hall, P. J. Sellers, and A. L. Marshak, "The interpretation of spectral vegetation indexes," *IEEE Transactions on Geoscience and Remote Sensing,* vol. 33, pp. 481-486, 1995.
[23] Z. Li, R. Hayward, J. Zhang, Y. Liu, and R. Walker, "Towards automatic tree crown detection and delineantion in spectral feature space using pcnn and morphological reconstruction," in *IEEE International Conference on Image Processing (ICIP)* Cairo, Egypt, 2009.
[24] M. Erikson, "Segmentation of individual tree crowns in colour aerial photographs using region growing supported by fuzzy rules," *Canadian Journal of Forest Research,* vol. 33, pp. 1557-1563, 2003.
[25] Z. Wang, Y. Ma, F. Cheng, and L. Yang, "Review of pulse-coupled neural networks," *Image and Vision Computing,* vol. 28, pp. 5-13, 2010.
[26] G. Kuntimad and H. Ranganath, "Perfect image segmentation using pulse coupled neural networks," *IEEE Transactions on Neural Networks,* vol. 10, pp. 591-598, 1999.
[27] R. D. Stewart, I. Fermin, and M. Opper, "Region growing with pulse-coupled neural networks: An alternative to seeded region growing," *IEEE Transactions on Neural Networks,* vol. 13, pp. 1557-1562, 2002.
[28] C. F. Jordan, "Derivation of leaf-area index from quality of light on the forest floor," *Ecology,* vol. 50, pp. 663-666, July 1969.
[29] "Code of practice for powerline clearance (vegetation)," Ergon Energy 2008.
[30] M. M. R. Mostafa and K.-P. Schwarz, "Digital image georeferencing from a multiple camera system by gps/ins," *ISPRS Journal of Photogrammetry and Remote Sensing,* vol. 56, pp. 1-12, 2001.
[31] J. Takaku and T. Tadono, "Prism on-orbit geometric calibration and dsm performance," *IEEE Transactions on Geoscience and Remote Sensing,* vol. 47, pp. 4060–4073, 12 Dec. 2009.
[32] R. Müller, M. Lehner, R. Müller, P. Reinartz, M. Schroeder, and B. Vollmer, "A program for dircet georeferencing of airborne and spaceborne line scanner images," *International Archives of Photogrammetry Remote Sensing and Spatial Information Sciences,* vol. 34, pp. 148-153, 2002.
[33] S. R. Mims, R. A. Kahn, C. M. Moroney, B. J. Gaitley, D. L. Nelson, and M. J. Garay, "Misr stereo heights of grassland fire smoke plumes in australia," *IEEE Transactions on Geoscience and Remote Sensing,* vol. 48, pp. 25-35, 2010.
[34] D. Scharstein and R. Szeliski, "A taxonomy and evaluation of dense two-frame stereo correspondence algorithms," *International Journal of Computer Vision,* vol. 47, pp. 7-42, 2002.
[35] Y. Boykov and V. Kolmogorov, "An experimental comparison of min-cut/max-flow algorithms for energy minimization in vision," *IEEE Transactions on Pattern Analysis and Machine Intelligence,* vol. 26, pp. 1124-1137, 2004.
[36] G. L. Gimel'farb, "Probabilistic regularisation and symmetry in binocular dynamic programming stereo," *Pattern Recognition Letters,* vol. 23, pp. 431-442, 2002.
[37] X. Yu, J. Hyyppä, H. Hyyppä, and M. Maltamo, "Effects of flight altitude on tree height estimation using airborne laser scanning.," in *Proceedings of the ISPRS working group VIII/2 'Laser scanners for forest and landscape assessment'*, Freiburg, Germany, 2004, pp. 96-101.
[38] T. Lindblad and J. M. Kinser, *Image processing using pulse-coupled neural networks*, Second ed.: Springer, 2005.
[39] M. Hirschmugl, M. Ofner, J. Raggam, and M. Schardt, "Single tree detection in very high resolution remote sensing data," *Remote Sensing of Environment,* vol. 110, pp. 533-544, 30 October 2007.

Steven J. Mills received the B.Eng. degree in aerospace avionics from Queensland University of Technology, Brisbane, Australia, in 2006. He is currently working toward the Ph.D. degree in image based visual servo control for unmanned aerials systems at the Australian Research Center for Aerospace Automation, Brisbane, Australia, since 2007. His research interests include robotics and automation, unmanned aerial systems, vision based control, automated inspection and image processing.

Marcos P. Gerardo received the B.E. degree in computing and electronic engineering in 2007 from CETYS Universidad, Mexico. He then undertook an internship at the German Aerospace Centre, Braunschweig, Germany, developing an onboard demonstrator for precise localization of trains. He also spent time in the semiconductor industry undertaking reliability analysis.

Currently he is a Research Fellow at the Australian Research Centre for Aerospace Automation (ARCAA). His main research activities include LiDAR data analysis, georeferencing and sensor evaluation.

Zhengrong Li received the B. Eng. (Hons) degree M. Eng. in 2003 and 2006 respectively from Northwest A&F University, China. He was appointed an assistant lecturer at the College of Information Engineering, Northwest A&F University since 2006. He is currently pursuing the Ph.D. degree at the Queensland University of Technology with the support of Cooperative Research Centre for Spatial Information (CRCSI). His research interests include image processing, pattern recognition and computational intelligence.

Jinhai Cai (M'05-SM'06) received the Ph.D. degree in computer science from University of Melbourne, Australia, in 2000. He worked in LH& Infotalk (Singapore) as a researcher between 1999 and 2001. He is currently working for Queensland University of Technology as a lecturer and senior research fellow since 2001. His research interests include computer vision, signal processing and pattern recognition.

Ross Hayward (M'00) received the B.Sc. degree from the Australian National University (ANU) in Canberra, Australia in 1983, a Graduate Diploma in Computer Science and a Phd. in connectionist systems from the Queensland University of Technology Brisbane, Australia in 1993 and 2001 respectively.

He has been a lecturer at QUT since 2002 teaching in the areas of artificial Intelligence, programming languages and computer architecture. He is also a member of the IEEE Computational Intelligence and Computer Societies and regularly organizes QUT's participation in the southeast Queensland computational intelligence chapter. His areas of interest include computer vision and machine learning for robotic platforms.

Luis Mejias (M'07) received the B.E. degree in electronics from the Universidad Nacional Experimental Politécnica, Barquisimeto, Venezuela, and the M.Sc. and Ph.D. degrees in telecommunication systems, and robotics and automation, respectively, from the Universidad Politécnica de Madrid, Madrid, Spain.

While completing the Ph.D. degree, he was leading the team in vision-guided unmanned aerial vehicle (UAV) for surveillance and visual inspection. He gained extensive experience in unmanned aerial vehicles and, in particular, autonomous helicopter platforms, investigating computer vision techniques for control and navigation. Dr. Mejias is currently a Lecturer in Aerospace Avionics at Queensland University of Technology (QUT), Brisbane, Australia, and Research Scientist in Unmanned Aerial Technologies at the Australian Research Center for Aerospace Automation at QUT.

Rodney A. Walker (M'01) was born in Cairns, Australia, in 1969. He received the B. Eng. degree in electronic systems and the B.App.Sc in computing from Queensland University of Technology in 1992. He completed his PhD in satellite navigation from the same institution in 1999 after spending a year studying at the Rutherford Appleton Laboratory in the UK. From 1998 to 2005 he was responsible for the GPS payload on Australia's Federation Satellite working closely with NASA JPL during this time. Since 2000 he has directed his interests to ICT in aviation and created the Australian Research Center for Aerospace Automation which now has over 30 full-time staff. He is also a private pilot with NVFR and Aerobatics endorsements.